Circuits as Resonators, Sensors, and Filters

David Barbosa
Department of Electrical and Systems Engineering
Washington University in St. Louis
St. Louis, USA
barbosa@wustl.edu

Paul Pham
Department of Electrical and Systems Engineering
Washington University in St. Louis
St. Louis, USA
p.h.pham@wustl.edu

***Abstract*—This report details the design and implementation of a linear dynamical system model in MATLAB to simulate and analyze the behavior of electrical circuits, specifically their effect on audio signals. This study establishes the discrete-time modeling technique by simulating basic RC and RL circuits, investigating model accuracy as a function of the sampling interval, h. The main RLC circuit model was derived, and its discrete-time response to a step input was investigated to explore how resistance (R), inductance (L), and capacitance (C) control oscillations and damping. Furthermore, the RLC model's frequency-domain characteristics are implemented to design three practical audio applications: [1] A resonator to emulate a tuning fork; [2] A sensor to isolate an 84 Hz rotor sound; and [3] a band-pass filter to remove unnecessary noise from a music file.**

I. Introduction

The ability to accurately model and predict analog electrical circuit behavior is a fundamental problem in the field of electrical engineering and signal processing, with applications ranging from wireless communication filters to audio equalizers [1]. The core problem lies in translating the real-world, continuous-time behavior of physical components into a discrete-time model that can be effectively simulated in MATLAB. This case study explores a solution to this challenge using a linear dynamical system:

$$\mathbf{x}_{k+1} = \mathbf{A}\mathbf{x}_k + \mathbf{B}\mathbf{u}_k \tag{1}$$

This series RLC circuit presents unique challenges for simulation. The complex interactions between the resistor, the inductor, and the capacitor create sophisticated behaviors like resonance, oscillation, and damping. Moreover, the model circuit's accuracy is critically dependent on the choice of the sampling step interval, h. An incorrect h can lead to an inaccurate or unstable simulation, failing to truly represent the physics of the circuit.

The goal is to build a robust circuit model that takes an arbitrary voltage signal, such as a step input or audio file, and accurately predicts the output voltage. Key stages to be successful include:

- Implement linear dynamical systems to model simple RC and RL circuits from first principles.
- Analyzing how the sampling interval, h, affects the accuracy and stability of the simulation.
- Derive matrices ($\mathbf{A}$ and $\mathbf{B}$) for the more complex RLC circuit model.
- Analyze the RLC circuit's time-domain reasons and its frequency-domain response.
- Designing and tuning the RLC model to compete in three audio-processing tasks: a resonator, a sensor, and a music filter.

This report details the methods used to derive and implement these models, presents simulation results, and discusses the implications of using linear systems for complex signal processing.

II. Methods

A. Modeling an RC circuit

The primary objective is to model a simple resistor-capacitor circuit (Appendix A (a)) and simulate the model's voltage response to a 1-volt DC step input using a discrete-time linear model. This was achieved by using the circuit's derived difference equation:

$$v_{C,k+1} = (1 - \frac{h}{RC})v_{C,k} + \frac{h}{RC}v_{\text{in},k} \tag{2}$$

Implementing this equation into MATLAB as a helper function `simRCvoltages`, the circuit was then simulated with $R = 1\ \text{k}\Omega$, $C = 1\mu\text{F}$, and a 1V step input, and lastly plotting the capacitor charging curve as shown in Figure 1.

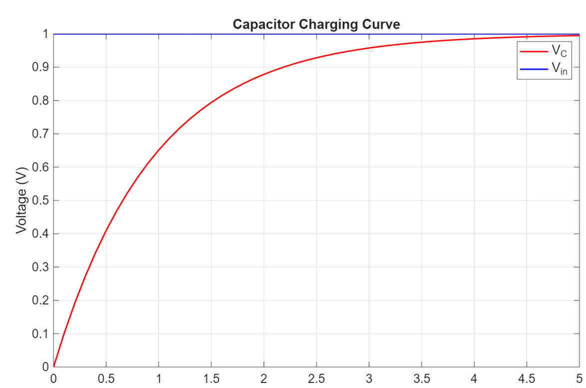

Fig. 1. Simulated RC circuit response to 1V step input. Capacitor voltage (v_C, red) charges from 0V toward 1V input (v_{in}, blue).

The key part of this analysis was to explore the effect of the sampling interval, h, on the model's accuracy. With the circuit's physical time constant being $\tau = RC = 0.001$s, the simulation was run with multiple iterations with different step sizes (h), and was then compared to the true theoretical charging curve:

$$v_C(t) = 1 - \exp(\frac{-t}{RC}) \quad (3)$$

Figure 2 illustrates how the sampling h critically affects the accuracy of the simulation. The "accurate" simulation using a small step size ($h = \tau/10 = 0.1$ms) is visually indistinguishable from the smooth, theoretical curve. The "large" step simulation ($h = \tau \times 5 = 0.5$ms) has a rougher line, and does not follow the theoretical curve as accurately, but remains to follow the general curve shape. The "inaccurate" simulation, using a step size too large ($h = 2.1 \times \tau = 2.1$ms), becomes numerically unstable – the voltage spikes to an impossible number and result.

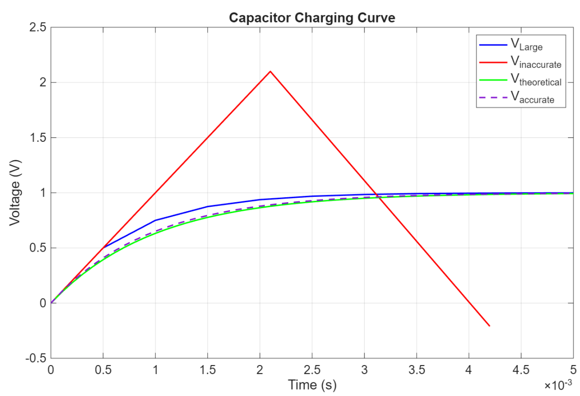

Fig. 2. RC circuit accuracy vs. time step h. Small h matches theory; large h causes instability.

The results of the findings demonstrate that the model is an approximation that assumes the circuit's state is constant during the interval h. When the step input is too large (specifically $h > 2\tau$), the assumption fails, and the error of each step compounds, leading to an unstable simulation. The behavior of the "real" capacitor (the theoretical curve) does not change; however, the only resultant is the accuracy of the model compared to the behavior of the "real" capacitor.

Lastly, this model confirms the physical meaning of the time constant τ. As shown in Figure 2, at $t = \tau = 0.001$s, the accurate capacitor voltage reaches approximately 0.632V. This verifies that τ is the time required for the capacitor to charge to approximately 63.2% of its final voltage.

B. Modeling an RL circuit

This section models a resistor-inductor (RL) circuit (Appendix A (b)), which serves as the complement to the RC circuit. In this configuration, the primary state variable solved for is the current (i) flowing through the circuit, as an inductor resists changes in current. The discrete-time equation for current is:

$$i_{k+1} = (1 - \frac{hR}{L})i_k + \frac{h}{L}v_{\text{in},k} \quad (4)$$

Implementing this equation as another helper function, `simRLvoltages`, the circuit was then simulated with the specified parameters of $R = 100\ \Omega$ and $L = 100$ mH (0.1 H). A new time constant, $\tau_{RL} = L/R = 0.001$s, is yielded with the new parameters, and an accurate sampling interval ($h = \tau_{RL}/10$) was used to simulate the circuit's response to a 1V step input.

Plotting the inductor charging curve (Figure 3) reveals a direct inverse of the resistor-capacitor circuit: the inductor voltage v_L starts at 1V (as it opposes the initial, sudden change in current) and then decays to 0V as the current becomes stable. As Figures 1 and 3 reveal, after the capacitor is fully charged, the steady-state voltage (v_C) converges at 1V. Similarly, in the RL circuit, after a long period of time, the steady-state voltage (v_L) converges at 0V, demonstrating the complementary nature of capacitors and inductors.

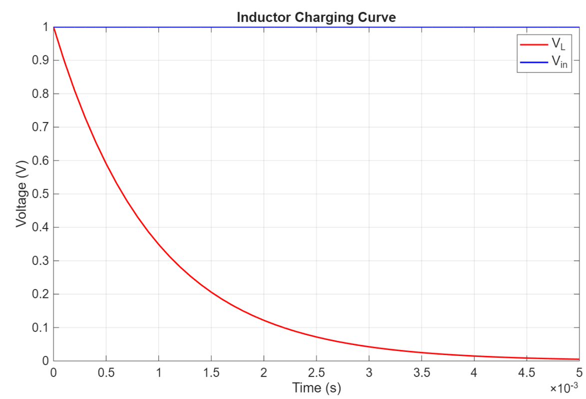

Fig. 3. RL circuit response to 1V step input. Inductor voltage (v_L, red) decays from 1V to 0V, while input (v_{in}, blue) remains at 1V

This complementary behavior is also seen in the steady-state current. For the steady-state current through the capacitor after it is fully charged, since v_C is a constant 1V and stops changing, this implies $dv/dt = 0$, meaning that the current would stop flowing ($i = 0$). The capacitor acts as an **open circuit**. Conversely, since the steady-state voltage across the inductor is 0V, this would mean that v_R would be 1V if v_{in} was equal to 1V, due to Kirchhoff's Voltage Law: $v_{\text{in}} - v_R - v_L = 0$. Using Ohm's Law ($v_R = i \times R$), substituting v_R and R solves for the steady-state current. This gives ($1 = i \times 100$), so the steady-state current through the inductor is $1/100$ A. The current flows freely, and the inductor acts as a **short circuit**.

C. RLC circuit analysis

In this section, we observe and model the combination of an inductor and a capacitor in a resistor-inductor-capacitor circuit (RLC circuit) (Appendix A (c)). In this particular circuit configuration, the primary state variables must be solved for the current (i) and the voltage across the capacitor (v_C). To model this particular design, a linear dynamical system (1) was taken to model the discrete-time equations for both the current and the voltage across the capacitor. To model this, the discrete-time equations (2), and (4) for both variables are coupled.

To ensure a numerically stable simulation, a semi-implicit Euler method is used. The resulting state space matrices A and B are for the system $\mathbf{x}_{k+1} = \mathbf{A}\mathbf{x}_k + \mathbf{B}u_k$ are derived as:

$$\mathbf{A} = \begin{bmatrix} 1 & \frac{h}{C} \\ -\frac{h}{L} & 1 - \frac{hR}{L} - \frac{h^2}{LC} \end{bmatrix}, \quad \mathbf{B} = \begin{bmatrix} 0 \\ \frac{h}{L} \end{bmatrix} \tag{5}$$

The full derivation of these matrices is detailed in the **Appendix**. With these defined variables, the linear dynamical system can be used to model a proper RLC circuit and demonstrate the changing values of the output voltage within the circuit. The values that primarily alter the RLC circuit are the inductance (L), resistance (R), and capacitance (C). Using MATLAB to simulate the linear dynamical system of an RLC circuit allows for an analysis of these changing values on the output voltage. Capacitance seems to inversely affect the oscillation frequency; increasing capacitance decreases the frequency. Inductance inversely affects the amplitude of the waveform, similar to capacitance. Resistance directly controls the voltage decay of the circuit; an increase in resistance indicates an increase in the decay.

To demonstrate the effects of resistance, the circuit was simulated using the MATLAB function `simRLCvoltages` with a 1V step input and a time interval of $h = \frac{1}{192000}$. Fixed parameters were set at $C = 0.1\mu$F and $L = 1$ mH. R was varied to show the different decay behaviors: $R = 100\ \Omega$ (slow decay), $R = 1000\ \Omega$ (fast decay), and $R = -150\ \Omega$ (Unstable decay).

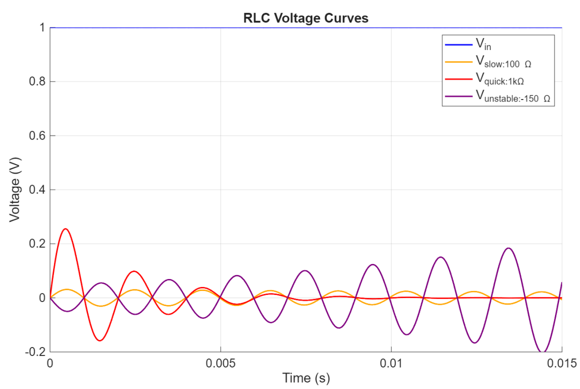

Fig. 4. RLC output (v_R) response to 1V step with varying R: slow decay (100Ω, orange), quick decay (1000Ω, red), and unstable growth (-150Ω, purple).

A 1V step input causes the model circuit to ring at its natural frequency. The audible sounds produced by these simulations correlate directly with these plots, with each different output of sound corresponding to its level of decay.

For the **Slow Decay** ($R = 100\ \Omega$), with low resistance, the circuit is underdamped. The voltage waveform shows a steady, gradual decay in amplitude. This matches the sound, which begins as a low-pitched "ping" and fades away, with a smaller "ping" heard immediately after the first. In contrast, the **Fast Decay scenario** ($R = 1000\ \Omega$) uses a high resistance, making the circuit overdamped. The plot shows an initial single, large oscillation (a "bump"), which is then immediately damped, causing the waveform to flatten out to nearly 0V. This corresponds to the sound, which is a single, sharp "thud" or "click" that is followed by silence. For the **Unstable Growth** ($R = -150\ \Omega$), with an imaginary, negative resistance, the plot shows the amplitudes increasing with every cycle. This matches the sound perfectly, which begins at a low volume and then rapidly increases in pitch and loudness as the simulation continues.

To understand how this RLC model circuit affects audio signals, its response to sinusoidal voltages at frequencies from 10 Hz to 10kHz was explored. Using the equation:

$$v_{\text{in}}(t) = \sin(2\pi f t)\ [\text{Volts}] \tag{6}$$

and the predefined components $R = 100\ \Omega$, $L = 100$ mH, and $C = 0.1\ \mu$F, a loop was run to simulate the circuit at various frequencies and systematically measure the steady-state output amplitude (v_R).

The simulation data shows that the output amplitude (voltage) heavily depends on the input frequency. At a low frequency of 10 Hz, the voltage output is small, close to zero. At 100 Hz, the amplitude is still minuscule (≈ 0.007 V). At 1000 Hz, however, the voltage output greatly increased, peaking at ≈ 0.12 V. At the highest frequency from the range, 10,000 Hz, the amplitude significantly drops back down to ≈ 0.019 V.

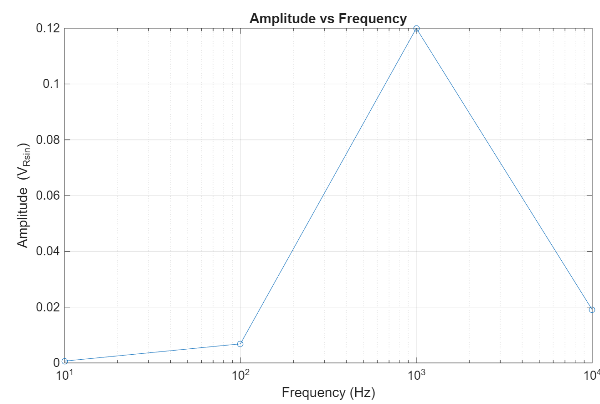

Fig. 5. RLC frequency response. Output amplitude V_R peaks in the mid-range, confirming band-pass behavior.

From our observations (see Figure 5), a conclusion was formed that the voltage output is small at the ends, and reaches a maximum peak somewhere in the middle of the frequencies (1000 - 1500 Hz). This showcases a **band-pass filter** [1], as it blocks very low and high frequencies (10 - 100 Hz and 10,000 Hz) and only allows a specific "band" of frequencies in the middle, where the amplitude is the highest.

This behavior correlates with what is heard. Small and large amplitudes, like amplitudes at 10 Hz and 10000 Hz, would sound very quiet or no sounds at all, while amplitudes near the peak or middle would be loud. Low, medium, and high frequencies correspond to low, medium, and high pitches, respectively, meaning that this band filter would "filter" out low and high pitches, only allowing mid-range sounds.

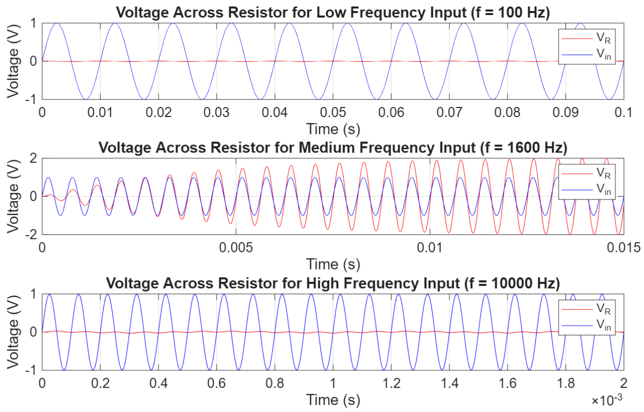

Fig. 6. Time-domain response to sinusoids. 100 Hz (top) and 10 kHz (bottom) are blocked; 1600 Hz resonant frequency (middle) passes.

III. Competition Designs and Methods

A. RLC design as a resonator

The RLC circuit was reconfigured to act as a resonator with a target frequency of 440 Hz and a decay time exceeding more than five seconds. To achieve this, several parameters and values were altered for this design.

The process for this configuration started with a chosen value of inductance that could simulate the target frequency, that being the inductance value of $L = 100$ mH (millihenries), a good value for a noise to simulate with sufficient volume. With the target frequency f and inductance L defined, the required capacitance C was calculated using the standard resonance formula:

$$f = \frac{1}{2\pi\sqrt{LC}} \tag{7}$$

Re-arranging to solve for C yields:

$$C = \frac{1}{((2\pi f)^2 L)} \tag{8}$$

Substituting the known values (f = 440 Hz, L = 0.1 H) into Equation (12) determines the required capacitance to be $C \approx 1.3\mu$F.

A long decay time requires minimal damping; therefore, a low resistance value of R = 0.05 Ω was selected. To model the long-term behavior and present the constant ringing, the simulation was designed to have a time interval to run for 15 seconds. A voltage pulse was then set to simulate the ringing over a period of time. These parameters allowed for analysis of the required input pulse voltage for the circuit to ring for more than 5 seconds, which appeared to be around -0.31 μV for a duration of about 5.2 μs.

B. RLC design as a sensor

The objective for this configuration is to isolate the 84 Hz rotor sound of the Mars rover "Ingenuity" flying on the surface of Mars from a noisy audio file. This requires designing the RLC circuit to act as a narrow band-pass filter centered at f = 84 Hz. The design was anchored with the particular capacitance value of C = 0.1 μF. The resonance formula (11) was then rearranged to solve for the inductance L required to achieve the target frequency:

$$L = \frac{1}{((2\pi f)^2 C)} \tag{9}$$

Substituting the known values (f = 84 Hz, C = 0.1 $\times 10^{-6}$ F) into Equation (13) yields the required inductance of $L \approx 35.9$ H.

Using the sampling interval $h \approx 5.2\mu$s to match the sampling rate of the audio file, the value of resistance was then set to a relatively low value (R = 100 Ω) to simulate the circuit properly.

C. RLC design as a filter

In order to configure the RLC circuit to act as a music filter, the primary aim was to remove unwanted noise sources, such as the 60 Hz "hum" and high-frequency "hiss," while preserving the core frequencies of the musical recording. To achieve this, a band-pass filter was designed utilizing the series RLC circuit, with the output voltage v_{out} taken across the resistor v_R.The design process began by defining the desired frequency pass-band. A lower cutoff frequency f_1 = 100 Hz and an upper cutoff frequency f_2 = 2000 Hz were established to capture the main musical content. [2] From these two values, the filter's central frequency $f_0 \approx 447.21$Hz was calculated using the geometric mean:

$$f_0 = \sqrt{f_1 f_2} \tag{10}$$

Subsequently, the bandwidth Δf= 1900 Hz of the filter was set as the difference between the upper and lower cutoff frequencies:

$$\Delta f = f_2 - f_1 \tag{11}$$

With the filter's frequency response specified, the component values were determined. Substituting the known values $f_0 \approx 447.21$Hz and the predetermined value C = 0.1 μF into the rearranged resonance formula for inductance (13) yields the required inductance $L \approx 1.267$ H.

Resistance R was calculated to match the desired bandwidth by rearranging the bandwidth formula:

$$\Delta f = \frac{R}{2\pi L} \tag{12}$$

To yield:

$$R = \Delta f \cdot 2\pi L \tag{13}$$

This set of parameter values ensures that the circuit passes the desired band of musical frequencies while attenuating the noise on either side of this band.

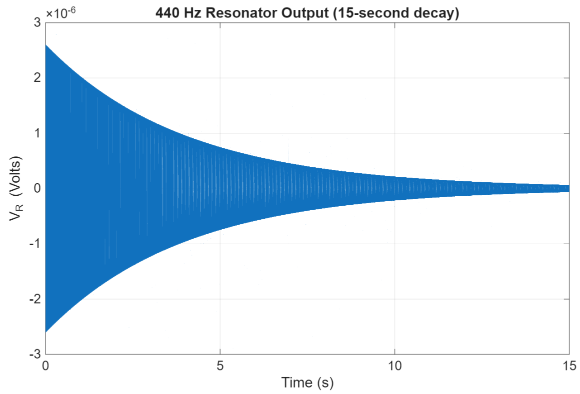

Fig. 7. 440 Hz resonator output. Voltage (v_R) rings for 15s with gradual decay.

IV. Circuit Performance and Discussion

A. Resonator Performance

The resonator design was successfully designed and emulated as a 440 Hz tuning fork. The output voltage of the circuit (Figure 7) highlights that when a 1V pulse is inputted, the circuit produces a visible sine wave.

The wave rapidly oscillates at the frequency $f = 440$ Hz, with its amplitude gradually decaying over 15 seconds. The slow decay is the direct result of the selected low resistance ($R = 0.05\ \Omega$), which minimizes the energy dissipation. The audio output confirms these results, producing a tone musically tuned to 'A4' that slowly fades in volume, just as a tuning fork would.

B. Sensor Performance

The RLC circuit performed effectively as a tuned sensor for the Mars Ingenuity Rover. Figure 8 compares the power spectrum of the original audio recording with the sensor circuit's output audio.

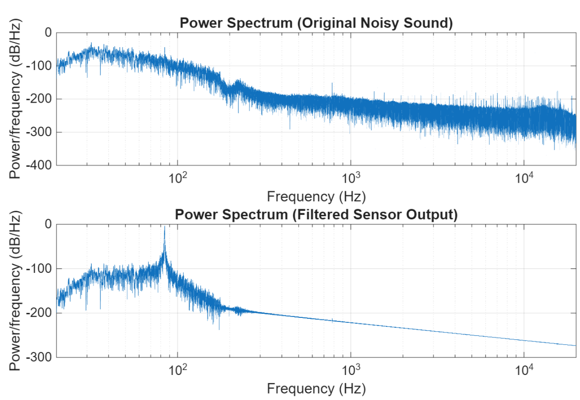

Fig. 8. Power spectra: Original Mars audio (top) vs. sensor output (bottom) isolating 84 Hz signal.

The original signal spectrum (top) is dominated by broadband noise at low frequencies (< 500 Hz), corresponding to the winds on Mars. The 84 Hz rotor signal is buried within the noise and is indistinguishable from the wind and other noises both visually and audibly. The filtered output spectrum (bottom) demonstrates the successful isolation of the target signal ($f = 84$ Hz). The circuit attenuates the broadband of wind noise significantly, leaving a distinct peak at $f = 84$ Hz, the rotor signal. Audibly, the recording is transformed from loud, noisy wind with the rotor nowhere to be heard, into a clear hum, successfully detecting the rover's presence.

C. Music Filter Performance

The performance of the RLC band-pass filter is demonstrated in Figure 9, which compares the power spectrum of the original signal to the filtered output.

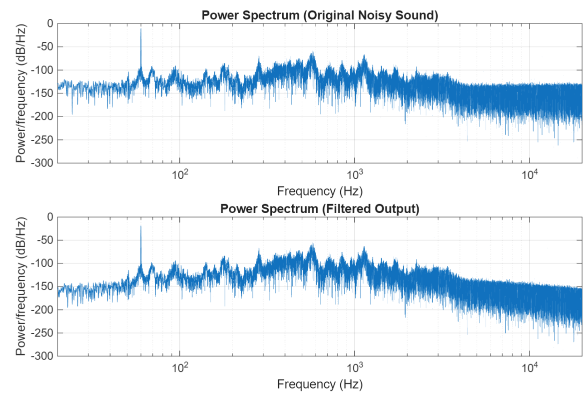

Fig. 9. Power spectra: Original noisy 'handel.mat' (top) vs. RLC band-pass filtered signal (bottom).

The original noisy sound spectrum (top) clearly displays the two target noise sources: a high amplitude spike at 60 Hz corresponding to the electrical "hum," and the wide band of "hiss" noises, visibly shown at the frequencies above ≈ 2000 Hz. The filtered output spectrum (bottom) confirms the filter's efficacy.

Due to low cutoff frequency of the filter ($f_1 = 100$ Hz), the 60 Hz spike is reduced. Conversely, the high-frequency hiss is visibly reduced, as the power spectrum decays significantly after the $f_2 = 2000$ Hz high cutoff. The content between 100 Hz and 2000 Hz is preserved, as the overall shape of the spectrum remains intact in both plots. Audibly, the prevalent hum and hiss are mostly removed without sacrificing volume and muffling the music, confirming the effectiveness of the band-pass filter design.

D. Limitations and Future Work

The main shortcoming of this approach is its absolute reliance on ideal components. Real-world resistors, inductors, and capacitors would have internal resistance or leakage, something that was not captured in our model. Furthermore, the discrete-time model relies on a fixed sampling h, which could lead to instability and inaccurate results if h is not small in relative to the circuit's time constant, as demonstrated in the RC circuit analysis.

Future work would include addressing these limitations. Implementing an adaptive step-size algorithm like the Runge-Kutta-Fehlberg method could ensure stability for any type of change without requiring a small global step interval [3]. Furthermore, incorporating real-world effects, such as voltage leakage, into the state-space matrices would enhance the model's realism. Lastly, designing higher-order filters by implementing multiple RLC stages could improve in sharpness of frequency cutoffs for audio applications.

V. Conclusion

This case study successfully demonstrated the development and application of a discrete-time dynamical system to model and simulate analog circuits for audio processing. The key findings are:

- The discrete-time modeling technique was established for simple RC and RL circuits and then extended to a more complex RLC model.
- Analysis confirmed the dependence of model accuracy and stability on the sampling interval, h, with inaccuracy occurring when h was too large relative to the time constant (e.g., $h > 2\tau$).
- The RLC model was successfully applied to three audio processing tasks: a 440 Hz resonating tuning fork, which ran stably for over 15 seconds, an 84 Hz sensor isolating the target "Ingenious" rover's hum and filtering out the broadband wind noise, and a band-pass filter that removed significant hum and hiss from a music file.

Overall, this project demonstrates how linear dynamical systems can serve as a powerful framework for simulating complex analog circuits, providing several useful insights into how the component values affect the outcomes in audio signal processing.

Appendix

A. Circuit Diagrams of RC, RL, RLC series circuits

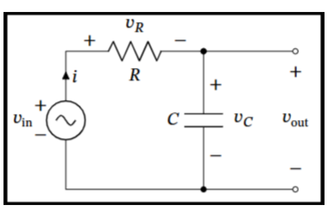

(a) Resistor-capacitor (RC) circuit

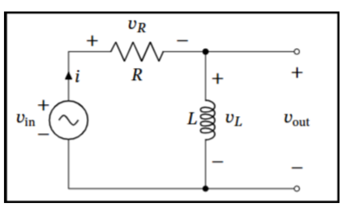

(b) Resistor-inductor (RL) circuit

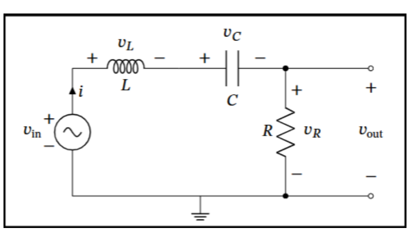

(c) Resistor-capacitor-inductor (RLC) circuit

Fig. 10. Circuit diagrams modeled.

B. Derivation of the Stable RLC State-Space Model

To model the RLC circuit stably, a semi-implicit Euler method is used. The state variables are v_C and i, with the update equations being:

$$v_{C,k+1} = v_{C,k} + \frac{h}{C} i_k \tag{14}$$

$$i_{k+1} = i_k + \frac{h}{L}\left(v_{in,k} - i_k R - v_{C,k+1}\right) \tag{15}$$

To find the explicit form $\mathbf{x}_{k+1} = \mathbf{A}\mathbf{x}_k + \mathbf{B}u_k$, we substitute Eq. (14) into Eq. (15):

$$i_{k+1} = i_k + \frac{h}{L} v_{in,k} - \frac{hR}{L} i_k - \frac{h}{L}\left[v_{C,k} + \frac{h}{C} i_k\right]$$

$$i_{k+1} = i_k + \frac{h}{L} v_{in,k} - \frac{hR}{L} i_k - \frac{h}{L} v_{C,k} - \frac{h^2}{LC} i_k$$

$$i_{k+1} = \left(-\frac{h}{L}\right) v_{C,k} + \left(1 - \frac{hR}{L} - \frac{h^2}{LC}\right) i_k + \left(\frac{h}{L} v_{in,k}\right)$$

From this, and Eq. (14), we construct the final matrices:

$$\mathbf{A} = \begin{bmatrix} 1 & \frac{h}{C} \\ -\frac{h}{L} & 1 - \frac{hR}{L} - \frac{h^2}{LC} \end{bmatrix}, \quad \mathbf{B} = \begin{bmatrix} 0 \\ \frac{h}{L} \end{bmatrix} \tag{16}$$

C. Contributions

David Barbosa contributed to the formulation of algorithms for RC, RL, and RLC circuits, as well as to testing and parameter setting for the sensor, resonator, and filter circuits. Additionally, he developed the analysis of the competition circuit and RLC circuit sections of the report. Furthermore, he developed parts of the derivation for the state-space matrices and implemented them into MATLAB as the RLC circuit, and developed parts of the design process for the circuits.

Paul Pham contributed to the formulation and implementation of the discrete-time linear models for the RC and RL circuits, as well as contributing to the analysis and discussion of how the sampling interval h affects model accuracy. Moreover, he contributed to the analysis and discussion of the RLC circuit's frequency response and its behavior as a band-pass filter. Furthermore, he contributed to the formatting, writing, and iterative revisions of this report.

References

[1] P. Prommee, P. Thongdit, and K. Angkeaw, "Log-domain high-order low-pass and band-pass filters," *International Journal of Electronics and Communications (AEÜ)*, vol. 79, pp. 234-242, Sep. 2017.

[2] K. Qian, "Comprehensive Analysis of Capacitance and Inductance Effect in the RLC Circuit Toward the Cut-off Frequency and Bandwidth," *Journal of Physics: Conference Series*, vol. 2419, no. 1, p. 012054, 2023.

[3] S. Paul, S. P. Mondal, and P. Bhattacharya, "Numerical solution of Lotka-Volterra prey-predator model by using Runge-Kutta Fehlberg method and Laplace Adomian decomposition method," Alexandria Engineering Journal, vol. 55, no. 1, pp. 613-617, Mar. 2016.